Solar Energy Materials & Solar Cells 152 (2016) 180–186

Contents lists available at ScienceDirect

Solar Energy Materials & Solar Cells

journal homepage: www.elsevier.com/locate/solmat

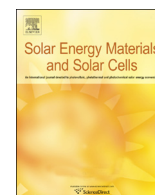

Influence of external contacting on electroluminescence and fill factor measurements

Hannes Höffler*, Jonas Haunschild, Stefan Rein

Fraunhofer Institute for Solar Energy Systems ISE, Heidenhofstr. 2, D-79110 Freiburg, Germany

ARTICLE INFO

Article history:
Received 5 January 2016
Received in revised form
30 March 2016
Accepted 31 March 2016
Available online 14 April 2016

Keywords:
Electroluminescence
Photoluminescence
Solar cells
Silicon
Fill factor

ABSTRACT

Electroluminescence imaging combined with photoluminescence imaging on solar cells allows extracting spatially resolved information on local solar cell quality. Numerous methods for the extraction of spatially resolved parameters have been introduced in the past. An important factor, which has mandatory influence on electroluminescence images, has not been discussed in detail yet. This factor is the influence of the external contacting scheme or erroneous contacting on the measurement results. In this work we discuss the influence of the external contacting scheme on the appearance of electroluminescence images and images of the spatially resolved series resistance which are calculated from electroluminescence images taken at different operating points. Furthermore we discuss the impact of erroneous contacting on fill factor measurements. We show that the impact of erroneous contacting on fill factor measurements becomes larger if busbar resistances become larger. The industrial trend towards thinner busbars with higher resistances hence motivates an electroluminescence based quality control for inline current voltage measurements of silicon solar cells.

© 2016 Elsevier B.V. All rights reserved.

1. Introduction

The combination of photoluminescence (PL) and electroluminescence (EL) imaging on silicon solar cells allows the extraction of information about the spatially resolved series resistance (R_s) of the cell. In the quantitative extraction of the spatially resolved series resistance was first suggested by Trupke et al. [1]. Michl et al. [2] investigated the reliability of the quantitative values by showing that the extracted values depend on the operating point at which the image is taken. In 2010 Glatthaar et al. [3] introduced a method called "coupled determination of dark saturation current density and series resistance" (C-DCR) similar to the one of Trupke et al., which additionally accounted for a distributed dark saturation current density as is the case in multicrystalline (mc) solar cells. In the following years numerous other works [4–10] dealt with the topic suggesting variations of the algorithms and investigating the underlying assumptions. Nevertheless none of these works focused on the influence of the external contacting scheme on the resulting images. The influence of the contacting scheme to EL images for the very special case of a certain grid design of interdigitated back contact (IBC) cells has been discussed by Schinke et al. [11]. The influence of external contacting on IV measurement result has been discussed in [12] without discussing EL imaging. Experience shows that the appearance of EL images and of the extracted images of the spatially resolved series resistance by any of the above methods depends on the external contacting scheme in a very sensitive way. Also erroneous contacting, meaning that one or more pins of the external contacting bars do not contact the busbar properly, which can e.g. be induced by pin abrasion, has significant impact on the appearance of EL images and can have significant impact on the measured fill factor in an IV measurement. As shown below the significance of different contacting schemes or erroneous contacting becomes larger if busbars become thinner and hence busbar resistances become higher. Due to high silver prices and higher efficiency potentials of solar cells with less shading of thick busbars the current trend in solar cell industry is towards thinner busbars and busbar plating [13], which additionally motivates a detailed discussion of measurement results depending on external contacting. In this work we introduce a simulation model to simulate EL and R_s images for different contacting scenarios. In Section 2 we give an instructive explanation of the equivalent circuit, which allows simulating EL and R_s images. In Section 3 we discuss different scenarios of external contacting schemes and possible erroneous contacting scenarios and compare the image contrasts induced by erroneous contacting to those induced by actual cell artifacts. In Section 4 we investigate the impact of erroneous contacting scenarios to the measured fill factor values.

* Corresponding author. Tel.: +49 761 4588 5651
E-mail address: hannes.hoeffler@ise.fraunhofer.de (H. Höffler).

http://dx.doi.org/10.1016/j.solmat.2016.03.039
0927-0248/© 2016 Elsevier B.V. All rights reserved.

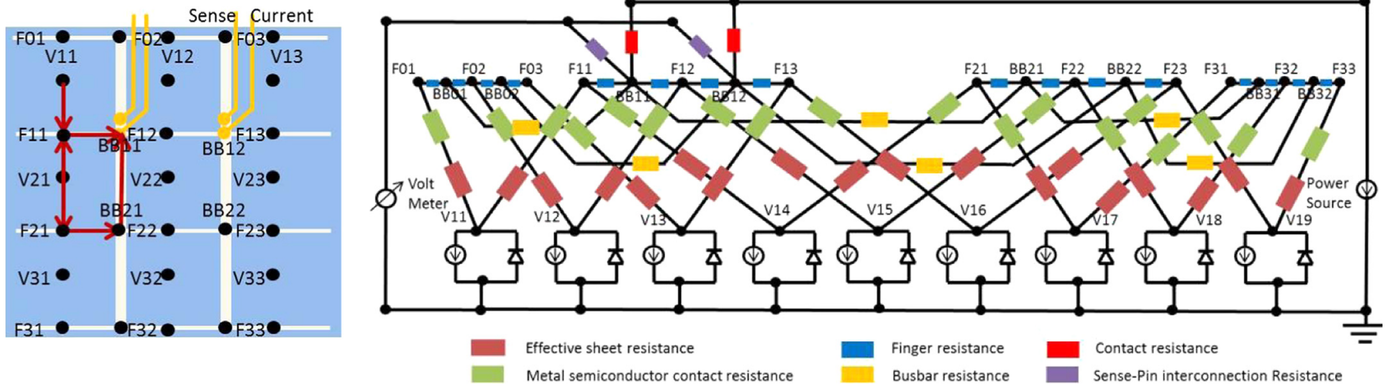

Fig. 1. (left) A schematic illustration of the solar cell's front side. The red arrows indicate the current path to the yellow external contacting unit. (right) Equivalent circuit of the solar cell in the instructive scenario. (For interpretation of the references to color in this figure legend, the reader is referred to the web version of this article.)

2. Instructive equivalent circuit scenario

For reasons of clarity we give an instructive scenario to the way EL images, R_s images and IV-curves are simulated taking into account the shape and the quality of the external contacting unit. For instructive purposes a very small (unrealistic) $3 \times 3\ \text{cm}^2$ solar cell is simulated featuring 4 fingers with 1 cm spacing and 2 busbars on the front side. This instructive scenario will be extended to large area $156 \times 156\ \text{mm}^2$ cells with realistic grids in the next section. In Fig. 1 schematic drawing of the solar cell's front side and the equivalent circuit, on which the simulation is based, are shown.

It is assumed that the current in the illuminated case is generated in each of the nine 'pixels' labeled with V_{xy} in Fig. 1. The current then travels either upwards or downwards to the points on the grid fingers labeled F_{xy} and passes through the effective sheet resistance $R_{sh,eff}$ (brown) and the metal–semiconductor contact resistance R_{ms} (green). The current then travels sideways through the finger resistances of the finger segments R_f (blue) to the points labeled BB*xy* on the busbars. To enter the external circuit it either directly passes through the contact resistances R_{cont} (red) or it needs to run through the resistance of one busbar segment R_{bb} (yellow) first. The current running sideways through the emitter from the 'pixels' directly to the busbars is neglected. This may seem unrealistic for the above scenario, but in realistic solar cells, where the busbar-busbar distance is much larger than the finger-finger distance, it is a reasonable assumption. In order to calculate the global voltage at the cell a 4-wire-measurement is simulated. It is assumed that the sense pins and the current pins are located at the same position. For the above scenario that means that the global voltage measured at the cell equals the arithmetic mean of the voltages at the points BB11 and BB12. To avoid currents flowing in between the sense pins the sense pins are assumed to be resistively coupled as it is common practice in IV-measurements. Sense-pin-interconnection-resistances (purple) are depicted in Fig. 1. The fact that the current generated in the lower part additionally has to pass resistances of the busbar segments results in an asymmetric voltage distribution across the cell and hence in asymmetric EL- and PL-images. The distribution of voltages across the points V_{xy} can be simulated for any operating point using e.g. the software LTspice, which is used in this work. Each of the local diodes' current sources is assumed to generate a current of $I_{sc} = \frac{j_{sc} * A}{N_{Pixels}}$, with j_{sc} being the short circuit current density, which we assume to be $38 \frac{\text{mA}}{\text{cm}^2}$, A being the cell area ($9\ \text{cm}^2$ in the above scenario) and N_{Pixels} being the number of 'pixels' (9 in the above scenario). Each diode is characterized by a dark saturation current density j_0 of $200 \frac{\text{fA}}{\text{cm}^2}$. Care has to be taken choosing the correct area weighted values for the ohmic resistances. For the effective sheet resistance we deviate $R_{sh,eff} = \frac{R_{sh}}{6} = 14\Omega$ (see Appendix A), with R_{sh} being the emitter sheet resistance (note that this is only valid if the 'pixels' are squares). We assume a typical emitter sheet resistance of $R_{sh} = 85\Omega/\text{sq}$ [14] for state of the art emitters. The metal–semiconductor contact resistance results from $R_{ms} = \frac{\rho_{ms}}{2 W_f L_f}$. With ρ_{ms} being the specific metal semiconductor contact resistance, which we assume to be $4\ \text{m}\Omega\ \text{cm}^2$ [14], W_f being the finger Width, which is assumed to be 60 μm and L_f being the length of the finger segment, which is 1 cm in the above scenario, that leads to $R_{ms} = 0.33\Omega$. The finger resistance of one finger segment calculates from $R_f = \frac{\rho_{paste} L_f}{W_f h_f}$. Note that for the instructive scenario the finger segment should also be considered gradually loaded and should hence (similar to the sheet resistance) be substituted by an effective finger segment resistance. Nevertheless this effect is negligible for realistic simulations with small finger segments as in Section 3. With ρ_{paste} being the specific resistance of the silver paste (35,000 μΩ μm), and h_f being the effective finger height, which is assumed to be 10 μm, the resulting value is $R_f = 0.5\Omega$. The busbar resistance analogously follows to $R_{bb} = \frac{\rho_{paste} L_{bb}}{W_{bb} * h_{bb}} = 0.05\Omega$, assuming values of $W_{bb} = 300\mu\text{m}$ and $h_{bb} = 20\mu\text{m}$. Note that the length of one finger segment L_f and the length of one busbar segment L_{bb} are equal due to our square model and depend on the number of 'pixels'. The parameter of major interest in this work is the contact resistance R_{cont},[1] which is the ohmic resistance between a current pin and the busbar, that the current has to pass through on the way from the busbar to the external circuit. In this work we assume a contact resistance of $10\ \text{m}\Omega$ for 'good' contacting. We will discuss different scenarios, in which single contact pins do not contact properly, which will simple be reflected in higher contact resistances.

In Fig. 2 results of the voltage distributions for the instructive scenario are shown. (a) and (b) show the voltage distributions for the illuminated case at operating points with 80% and 90% of the short circuit current extracted respectively. Charge carriers are generated in the 'pixels' and induce a voltage at the pn-junction. Depending on the 'pixel' the charge carriers have to pass through different resistances until they leave into the external current. This leads to voltage drops at the resistances shown in Fig. 1. These voltage drops depend on the amount of current flowing through each of the resistances. This is the reason why the voltage differences in the case of 90% current extraction are higher than in the case of 80% current extraction. In the EL case the charge carriers are injected at the points of the contacting pins. Hence the voltage

[1] In photovoltaics the term contact resistance usually refers to the metal semiconductor contact resistance. In this work the term contact resistance refers to the ohmic resistance between current pin and busbar. We explicitly speak of the metal semiconductor contact resistance if referred to.

Download English Version:

https://daneshyari.com/en/article/77593

Download Persian Version:

https://daneshyari.com/article/77593

Daneshyari.com